Proceedings of the 1991 IEEE
International Conference on Robotics and Automation
Sacramento, California - April 1991

Avoiding Stick-Slip in Position and Force Control Through Feedback *

Pierre E. Dupont

Department of Aerospace and Mechanical Engineering
Boston University, Boston, MA 02215

Abstract

This paper discusses the avoidance of stick-slip motion at low velocities through feedback control. Simplified single-joint robot models are derived for position and force control. It is shown that both models can be represented by the same differential equation. Most prior work in control has used friction models which depend only on the current value of velocity. This type of analysis indicates that stick-slip can be avoided only through velocity feedback. The tribology literature, however, indicates that friction also depends on the past history of motion. To include this dependence, a state variable friction model is used in conjunction with the position and force control models. Analysis reveals the existence of a second regime of stable, low-velocity motion associated with position feedback gains above a critical value. This is an important result because the accuracy of position data is typically much better than that of velocity data at these speeds.

1 Introduction

The effect of friction on robot performance has been demonstrated by a number of researchers [1,4]. Its effect is perhaps most noticeable at very low velocities. At these speeds, motion tends to be intermittent. Commonly referred to as stick-slip, intermittent motion can lead to overshoot and large-amplitude limit cycling.

This paper addresses the question of how to achieve stable force and position control at very low velocities. The answer to this question depends critically on the friction model.

In the next section, friction modeling is discussed. State variable models which include the transient effects of friction are introduced. In Section 3, simplified robot models are derived for position and force control. Section 4 includes a stability analysis of the force and position control models incorporating a linearized state variable friction law. The stability criteria are compared with those obtained using a friction law which depends only on current velocity. Section 5 discusses the implications of this analysis for the control of steady, low-velocity motion.

*This work was supported by the IBM Corporation through a Postdoctoral Fellowship and by the U.S. Army Research Office under grant DAAL03-89-K-0112.

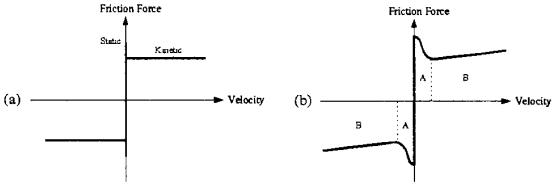

Figure 1: Friction Force Versus Velocity. (a) Kinetic / Static Model. (b) Complex Model.

2 Friction Modeling

Contrary to what is taught in introductory physics, the friction force for steady sliding is a continuous function of velocity - at least as long as the direction of relative motion is not reversed. The slope of this curve depends on the composition of the materials and any lubricant between them.

The characteristic friction-velocity curve for hard materials separated by liquid lubricants is contrasted with the static-kinetic model in Figure 1. For liquid lubricants, this curve is usually referred to as the Stribeck curve. For the range of low velocities labeled A, the curve can have a steep negative slope.

It is important to note that friction-velocity curves, including Stribeck curves, represent friction behavior for *steady sliding*. Sampson et al [10] were among the first to note the multi-valued behavior of friction. Friction is not determined by current velocity alone; it also depends on the past history of motion. This functional relationship for the friction, f, can be expressed as

$$f(t) = \mathcal{F}[V(t), \sigma_n(t); V(\tau), \sigma_n(\tau)], \; -\infty < \tau < t \qquad (1)$$

in which V denotes velocity and σ_n, normal stress.

In a control context, Dahl [3] and Walrath [12] developed transient models for friction and stiffness in ball bearings oscillating about zero velocity. However, their steady-state friction-velocity curves were flat. They observed a constant Coulomb friction level dependent only on the sign of velocity. Their models' transient response resulted only from velocity reversals. Since it has been demonstrated that steady-state robot friction is similar to Figure 1(b) (see [1]), these models are inadequate for our purposes.

Independent of the tribological community, researchers in earthquake prediction suggested that earthquakes are stick-slip events due to the relative motion of the earth's crustal plates. As a result, Ruina and others have worked on the experimental and theoretical development of constitutive friction relations [9]. Their experiments were performed on rock samples with and without "lubricants". These relations are referred to as *state variable friction models.*

The state variable friction laws proposed in the literature typically possess the following three properties (assuming constant normal stress):

(1) A Steady-state Dependence on Velocity.

(2) An Instantaneous Dependence on Velocity.

(3) Characteristic Slip Distances.

The steady-state effect, (1), represents what we have been calling the friction-velocity or Stribeck curve. The instantaneous effect, (2), means that an instantaneous change in velocity results in an instantaneous change in the friction force *in the same direction.* The third property indicates that following a sudden change in velocity, the steady-state curve is approached through an exponential decay over characteristic slip distances. For constant normal stress, the general model including the n state variables, θ_i is given by

$$f = f(V, \theta_1, \theta_2, \ldots, \theta_n) \quad (2)$$

$$\dot{\theta}_i = g_i(V, \theta_1, \theta_2, \ldots, \theta_n), \quad i = 1, 2, \ldots, n \quad (3)$$

This form implies that a sudden change in velocity cannot produce a sudden change in the state, θ, but does affect its time derivative. Hence, the direct velocity effect takes place at constant state. The steady-state friction-velocity curve can be obtained by setting the g_i equal to zero and substituting the resulting values for θ_i into f. A very simple law of this type containing a single state variable is [9]:

$$f = f_0 + A\ln(V/V_0) + \theta \quad (4)$$

$$\dot{\theta} = -\frac{V}{L}[\theta + B\ln(V/V_0)] \quad (5)$$

L is a characteristic length controlling the evolution of the state. The pair (V_0, f_0) corresponds to any convenient point on the steady-state friction-velocity curve. In this case, the steady-state curve is given by

$$f_{ss}(V) = f_0 + (A - B)\ln(V/V_0) \quad (6)$$

The functional form of this and other state variable models was deduced from the response to step changes imposed on the velocity at the friction interface. The fact that very small, steady velocities were achieved through closed-loop control in these experiments indicates that stable, low-velocity control is possible - at least for rocks. The response to step changes in velocity for this simple state variable law are depicted in Figure 2.

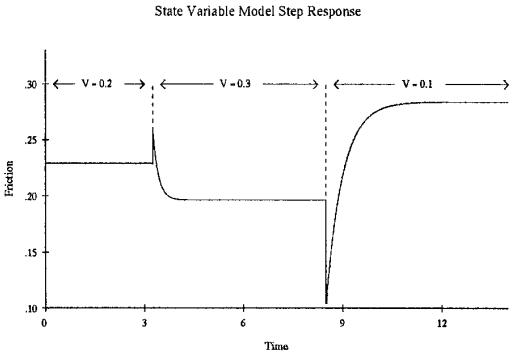

Figure 2: Response to Step Changes in Velocity: Single State Variable Model.

Many steady-state laws appearing in the literature represent the transition from static to kinetic friction by a term exponential in velocity. A general model of this form including Coulomb and viscous friction is:

$$f(V) = \left[c_0 + c_1 V + c_2 e^{-(V/c_3)^{c_4}}\right] \mathrm{sgn}(V) \quad (7)$$

with constants $c_0, \ldots, c_4 > 0$. Note that the state variable models were specifically developed to model low velocity effects while steady-state laws are formulated to fit the entire velocity operating range.

The state variable friction laws were developed from experiments involving sliding rocks using only substances such as water and gouge as lubricants. It is reasonable to question their applicability to lubricated machine parts. Strong motivation for the state variable models is provided by the experiments of Hess & Soom measuring friction for an oscillating velocity of constant sign [6]. They found that as the amplitude of oscillation increased, the friction-velocity curve became a closed loop centered around the steady-state friction curve.

While Hess & Soom modeled this behavior by introducing a simple time delay in their steady-state equation, the simulated response of a state variable law (shown in Figure 3) compares favorably in shape with Hess & Soom's experimental plots. Thus their experiments confirm that transient friction behavior can occur in conventional lubricated systems and suggest that it may be of the type represented by state variable friction laws. Similar experiments involving velocity steps are needed to confirm the applicability of the state variable laws, in particular, to confirm the existence of a direct velocity effect.

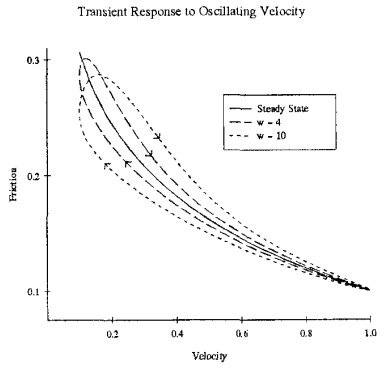

Figure 3: Response of State Variable Friction Law to an Oscillating Velocity, $V = V_0 + V_1 \sin(wt)$, $V_0 > V_1$. For this set of parameters, $w = 1$ traces out the steady-state curve shown.

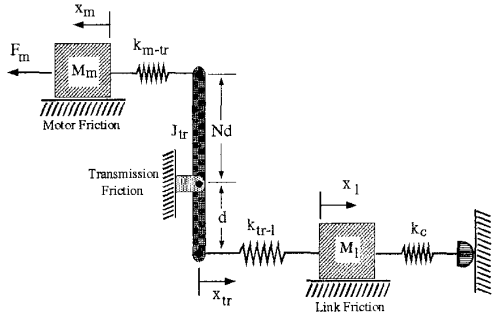

Figure 4: Lumped Parameter Model of Single Robot Joint.

3 Robot Modeling

The lumped parameter model for the motion of a single robot joint is shown in Figure 4. This model has three inertia elements for the motor, transmission and link. Associated with each inertia element is a friction force or torque arising from the relative motion between an element and its supports. Each inertia element is connected to its neighbor(s) by a spring. In the case of force control, the contact between the link element and the environment has an associated stiffness, k_c. A lever is used to represent a transmission with a reduction ratio of $N : 1$.

The transmission can be eliminated from Figure 4 to get the mass-spring model of Figure 5 by using the following transformations.

$$M'_m = N^2 M_m \qquad M_{tr} = J_{tr}/d^2$$
$$F'_m = N F_m \qquad f_m = f_m(N x'_m, N \dot{x}'_m, \ldots)$$
$$x'_m = x_m/N \qquad k'_{m-tr} = N^2 k_{m-tr}$$

While these transformations hold only for small displacements of the depicted transmission, in general, they hold

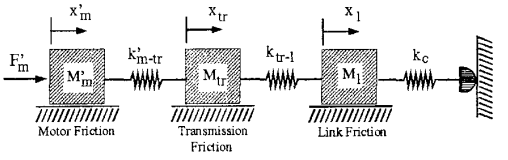

Figure 5: Mass-Spring Model Obtained by Transforming Parameters to Account for Transmission Ratio.

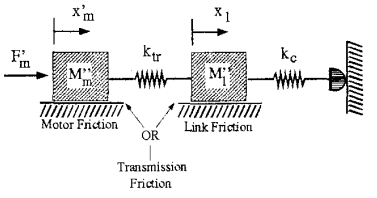

Figure 6: Simplified Model Obtained by Placing the Transmission at the Motor or the Joint.

for arbitrary displacements of an actual transmission. Note that motor friction is computed as a function of the original motor displacement, x_m, and its time derivatives.

If speed reduction occurs at the motor or the joint, either k_{m-tr} or k_{tr-l}, respectively, is very large compared to the other stiffnesses. For these cases, the transmission inertia can be combined with that of the motor or link, respectively.

As noted by Townsend, placing the transmission at the joint makes for a stiffer transmission and maximizes open-loop position bandwidth [11]. In either case, the model simplifies to that of Figure 6 using the following transformations.

Transmission at Motor	Transmission at Joint
$k_{tr} = k'_{tr-l}$	$k_{tr} = k'_{m-tr}$
$M''_m = M'_m + M_{tr}$	$M''_m = M'_m$
$M''_l = M'_l$	$M''_l = M'_l + M_{tr}$
$f_m = f_m + f_{tr}$	$f_l = f_l + f_{tr}$

One further simplification is made to obtain a single model which can be used for investigating the low-velocity stability of both position and force control. It is assumed that a high-gain, servo-controlled motor capable of both torque and velocity control is used. It is assumed that motor friction is small compared to the rest of the system and that servo feedback is sufficient to produce a steady output force or position trajectory. (This implicitly assumes that high-gain feedback can stabilize low-velocity friction in very stiff systems. Later analysis will show this to be true.)

For position control, this assumption means that the motor can produce a displacement, x_m, and the model reduces to what is shown in Figure 7(a). For force control, we take the motor output as the the force, F_m, and

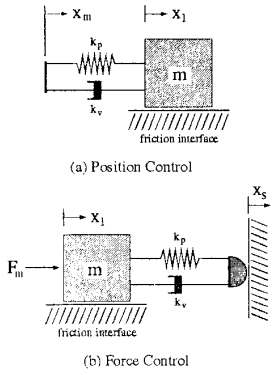

Figure 7: Models for Testing the Stability of Low-Velocity Motion for Position and Force Control. They assume the motor can be regarded as a position or force source, respectively.

make the further assumption that contact stiffness is much smaller than transmission stiffness or $k_c << k_{tr}$. The force-control model appears as Figure 7(b). (In Figure 7, we have dropped the prime on x_m and substituted m for M_l''.) The springs in these models represent the inherent stiffness of the mechanism. In order to introduce viscous damping, the dashpots shown in Figure 7 have been added. The parallel spring and dashpot of Figure 7(b) can be viewed as a visco-elastic finger.

These are the simplest models incorporating both friction and flexibility. Note that the force control model is similar to one used by Armstrong to analyze open-loop, force-control experiments on a PUMA robot [2].

As will be shown, the models in Figure 7 are equivalent for obtaining bounds on feedback gains for steady sliding. Consider first the position-control model of Figure 7(a). Summing forces on the mass, m,

$$m\ddot{x}_l = k_v(\dot{x}_m - \dot{x}_l) + k_p(x_m - x_l) - f + d(t) \qquad (8)$$

Under the assumption of steady motor motion, $\dot{x}_m = V_0$. In the absence of disturbances, $d(t)$, the steady-state solution yields a spring displacement, δ_{ss}.

$$\delta_{ss} = f_{ss}(V_0)/k_p$$

With disturbances, $\dot{x}_l$ is perturbed from steady sliding,

$$\dot{x}_l(t) = V_0 + \dot{x}(t),\ \dot{x}(t) << V_0$$

and the resulting dynamic equation is

$$m\ddot{x} + k_v\dot{x} + k_p x + (f - f_{ss}(V_0)) = d(t) \qquad (9)$$

In this formulation, k_p and k_v are the inherent stiffness and damping of the transmission. They can also be interpreted as feedback gains.

Now consider the force control model in Figure 7(b). If $x_s = 0$ represents the displacement of the surface, summing forces yields the following.

$$m\ddot{x}_l = F_m + d(t) - f - k_v\dot{x}_l - k_p x_l \qquad (10)$$

Let $\dot{x}_l(t) = V_0 + \dot{x}(t)$ as before. The dynamic equation is the same as that obtained for position control, namely, (9).

4 Linearized Friction Analysis

Consider the class of friction laws which depend on the current velocity and slip history assuming constant normal stress.

$$f(t) = \mathcal{F}[V(t); V(\tau)],\ -\infty < \tau < t \qquad (11)$$

Assume that f can be separated into an instantaneous rate-dependent component and an evolutionary component. The latter tends toward a steady-state value for sufficient slip at a particular velocity. In the systems of interest, the slope of the steady-state friction-velocity curve is negative for a range of low velocities.

$$\frac{df_{ss}(V)}{dV} < 0$$

Following Rice and Ruina [8], the impulse response will be used to represent the linearized behavior of $f(t)$ around the equilibrium point, $f_{ss}[V_0]$.

$$f(t) = f_{ss}[V_0] + \int_0^t h(t-\tau)V(\tau)d\tau \qquad (12)$$

Recognizing that the direct velocity effect is an impulse function, we can take it out of the convolution integral,

$$f(t) = f_{ss}[V_0] + f_v V(t) - \int_0^t g(t-\tau)V(\tau)d\tau \qquad (13)$$

in which f_v and $g(t)$ are dependent on V_0. From this equation, the instantaneous rate of change of friction with velocity is given by

$$\frac{\partial f(V)}{\partial V} = f_v \qquad (14)$$

and the steady-state change of friction with velocity is

$$\frac{df_{ss}(V)}{dV} = f_v - \int_0^\infty g(t)dt \qquad (15)$$

Experiments indicate that the instantaneous dependence of friction on velocity is positive and so $f_v > 0$. For the case of negatively-sloped, steady-state friction curves,

$$f_v < \int_0^\infty g(t)dt \qquad (16)$$

The following conditions are imposed on $g(t)$.

$$g(0) = 0 \qquad g(t) \geq 0 \qquad (17)$$

The condition $g(t) \geq 0$ ensures that the overall decay is monotonic.

Inserting this equation into (9), the dynamic equation for position and force control, yields

$$m\ddot{x} + k_p x + (k_v + f_v)\dot{x} - \int_0^t g(t-\tau)\dot{x}(\tau)d\tau = d(t) \quad (18)$$

Taking the Laplace transform of $x(t)$ and solving for $X(s)$,

$$X(s) = \frac{D(s)}{ms^2 + (k_v + f_v - G(s))s + k_p}. \quad (19)$$

Consider for a moment the simpler friction law, $f = f(V(t))$. In this case,

$$f_v = \frac{\partial f}{\partial V}(V_0) \quad (20)$$

Stability is determined by the locations of the poles of $X(s)$ which for this simpler case are the roots of

$$ms^2 + (f_v + k_v)s + k_p = 0 \quad (21)$$

Since $m > 0$, instability will occur if $(f_v + k_v) < 0$. If the friction law is negatively sloped at V_0 then additional damping, k_v, is needed to achieve stability. The value of k_v can be selected as the minimum value of $k_v = -f_v(V)$ for $0 \leq V < V_{max}$ to achieve asymptotic stability over the whole range of velocities. In this linear analysis, the only requirement on k_p for stability is that $k_p > 0$.

For example, consider the friction law

$$f(V) = c_0 + c_1 V + c_2 e^{-(V/c_3)^2} \quad (22)$$

In this case,

$$f_v = \frac{\partial f}{\partial V} = c_1 - \frac{2c_2 V}{c_3^2} e^{-(V/c_3)^2} \quad (23)$$

If $f_v < 0$, a positive k_v is needed to stabilize the system. The hardest velocity to stabilize (requiring the maximum k_v) is found using

$$\frac{\partial f_v}{\partial V} = 0 \quad (24)$$

to be

$$V_{cr} = \frac{c_3}{\sqrt{2}} \quad (25)$$

For asymptotic stability, $k_v > -f_v(V_{cr})$ where

$$f_v(V_{cr}) = c_1 - \frac{\sqrt{2}c_2}{c_3} e^{-1/2} \quad (26)$$

Let us return to analyzing the feedback gains necessary to stabilize (19). Since G(s) can take on complex values, the analysis of the pole locations of $X(s)$ for this system is more involved. Following the derivation in [8], a root locus for k_p is constructed while holding k_v fixed. Consider the roots of the following.

$$ms^2 + (k_v + f_v - G(s)) + k_p = 0 \quad (27)$$

For $Re(s) > 0$, $G(s)$ is bounded since its integral over time is bounded (see (15)) and, in the limit, $G(s \to \infty) = 0$. Let us consider all possible values of k_p starting with $k_p \to \infty$. For the preceding equation to be true with $Re(s) > 0$, s must go to infinity. Since $G(\infty) = 0$, the real part of the solution is

$$Re(s) = \frac{-(f_v + k_v)}{2m} \quad (28)$$

Since f_v and k_v are both positive, this is a contradiction and so (27) has no unstable roots for $k_p \to \infty$.

Now consider when $k_p = 0$. If our fixed value of k_v satisfies

$$k_v + f_v - \int_0^\infty g(t)dt < 0 \quad (29)$$

then there is at least one positive real root in this case since

$$ms^2 + (k_v + f_v - G(s))s \quad (30)$$

is negative for small real s and positive for large real s. This follows from continuity since

$$k_v + f_v - G(0) = k_v + f_v - \int_0^\infty g(t)dt < 0 \quad (31)$$

$$k_v + f_v - G(\infty) = k_v + f_v > 0. \quad (32)$$

So as k_p goes from infinity to zero, a root, or pair of roots, must cross the imaginary axis. Substituting $s = 0$ and $s = \pm i\infty$ into (27) show that these are not solutions since m, f_v, k_v and k_p are all positive. The remaining possibility is a pair of imaginary roots, $\pm i\omega$ associated with a critical value of k_p.

$$-m\omega^2 \pm i\omega(k_v + f_v - G(\pm i\omega)) + k_{cr} = 0 \quad (33)$$

Separating this equation into real and imaginary components gives the following equations for ω and k_{cr}.

$$k_v + f_v = \int_0^\infty g(t)\cos(\omega t)dt \quad (34)$$

$$k_{cr} = m\omega^2 + \omega \int_0^\infty g(t)\sin(\omega t)dt \quad (35)$$

Using our assumption that $g(t) \geq 0$ and noting that

$$\int_0^\infty g(t)dt \geq \int_0^\infty g(t)\cos(\omega t)dt \quad (36)$$

we see that (35) has a solution only if

$$k_v + \frac{df_{ss}(V)}{dV} = k_v + f_v - \int_0^\infty g(t)dt < 0 \quad (37)$$

The stability results are summarized below.

- For a friction law of the form $f = f[V(t)]$, asymptotic stability is achieved for:

$$k_v > -f_v(V_0) \text{ and } k_p > 0.$$

- For a friction law of the form $f = f[V(\tau), -\infty < \tau \leq t]$, asymptotic stability is achieved for:

$$(f_v + k_v) > \int_0^\infty g(t)dt \text{ and } k_p > 0.$$

OR

$$(f_v + k_v) < \int_0^\infty g(t)dt \text{ and } k_p > k_{cr}.$$

Nonlinear analyses of friction laws with one and two state variables appear in Gu et al [5].

5 Implications for Robot Control

In deriving the equations for our models, we interpreted k_v and k_p as the inherent damping and stiffness of the system. Of course, we can also interpret them as the feedback gains of our controller. In this light, what the preceding analysis has shown is that velocity feedback is not the only way to stabilize a system with a negatively-sloped steady-state friction-velocity curve. Analysis of state variable friction models, which include the transient effects of friction, reveals that sufficiently stiff systems will also be stable.

Recognizing the effect of stiffness on stable sliding is not a new result. Rabinowicz noted with surprise in 1951 that by increasing damping or stiffness, not only could the amplitude of stick-slip be reduced, in many cases it could be eliminated entirely [7].

A robotic demonstration of the stability of stiff systems may be reflected in the experimental results of Armstrong [1]. He found he could obtain very small velocities open loop by applying current ramps to the first joint motor of a PUMA robot while it pressed against a hard surface through a spring. Stiffer springs yielded smaller velocities. He reports stick-slip for the negatively-sloped region of the friction-velocity curve for all but the very lowest velocities obtained. These points were, of course, obtained using the stiffest springs. Using a friction model dependent only on current velocity (such as (22)), the amount of damping necessary for stability falls off as zero velocity is approached. (See (23).) Even so, Armstrong reports that these points should require substantially higher damping for stability than was observed. In the context of a state variable friction law, however, the stability of these points is due to the large stiffness of the springs used to obtain these very low velocities.

The actual choice of stabilization through k_p or k_v will depend on the friction law and the accuracy and cost of available sensors. The optimal choice may include both position and velocity feedback since increasing k_v decreases the critical value of k_p. (See (35).) With current sensor technology, stabilization through position feedback may be best since position data can be accurately and directly obtained using position and force sensors (typically, $\sigma^2(x) << \sigma^2(\dot{x})$).

6 Conclusion

The ability to achieve steady, low-velocity motion is important for robots as well as for any machines with tasks involving fine positioning or force control. In practice, however, the highly nonlinear behavior of friction near zero velocity imposes a minimum stable velocity below which stick-slip occurs. This places a limit on position and force resolution. In addition, the overshoot associated with limit cycling can lead to task failure.

In this paper, we have explored the ramifications of transient friction behavior as expressed by state variable friction laws for the control of steady, low-velocity motion. While friction laws which neglect transient effects predict stable sliding only through velocity feedback, our analysis indicates that steady motion can be obtained through position feedback as well. This is an important result since sensor-derived position data is typically much more accurate than velocity data.

While the state variable friction laws were developed to explain rock friction, there is sufficient evidence to suggest that similar laws hold for friction between lubricated metals. To confirm the ideas in this paper, experimental work is needed on two fronts: (1) determining state variable friction laws for lubricated metals and (2) applying these results to robot control.

Acknowledgement

I would like to thank James Rice for the helpful discussions of state variable friction laws.

7 References

1. B. Armstrong, "Friction: Experimental Determination, Modeling and Compensation." *Proceedings 1988 IEEE Int. Robotics and Automation Conf.*, Philadelphia, PA, April, 1988.
2. B. Armstrong-Helouvry, "Stick-Slip Arising From Stribeck Friction." *Proceedings 1990 IEEE Int. Robotics and Automation Conf.*, Cincinnati, OH, May, 1990.
3. P.R. Dahl, "Measurement of Solid Friction Parameters of Ball Bearings." *Proc. of 6th Annual Symp. on Incremental Motion Control Systems and Devices*, University of Illinois, 1977.
4. P. Dupont, "Friction Modeling in Dynamic Robot Simulation." *Proceedings 1990 IEEE Int. Robotics and Automation Conf.*, Cincinnati, OH, May, 1990.
5. J. Gu, J. Rice, A. Ruina and S. Tse, "Slip Motion and Stability of a Single Degree of Freedom Elastic System with Rate and State Dependent Friction." *J. Mech. Phys. Solids*, Vol. 32, No. 3, 1984.
6. D. Hess and A. Soom, "Friction at a Lubricated Line Contact Operating at Oscillating Sliding Velocities." *ASME Journal of Tribology*, Volume 112, January 1990.
7. E. Rabinowicz, "A Study of the Stick-Slip Process." *Friction and Wear*, Editor Robert Davies, Elsevier Publishing Co., New York, 1959.
8. J. Rice and A. Ruina, "Stability of Steady Frictional Slipping." *Journal of Applied Mechanics*, Volume 50, June 1983.
9. A. Ruina, "Friction Laws and Instabilities: A Quasistatic Analysis of Some Dry Frictional Behavior." Ph.D. Dissertation, Division of Engineering, Brown University, 1980.
10. J. Sampson, F. Morgan et al, "Friction Behavior During the Slip Portion of the Stick-Slip Process." *Journal of Applied Physics*, Volume 14, December 1943.
11. W. Townsend and K. Salisbury, "Mechanical Bandwidth as a Guideline to High-Performance Manipulator Design." *Proceedings 1989 IEEE Int. Robotics and Automation Conf.*, Scottsdale, April, 1989.
12. C. Walrath, "Adaptive Bearing Friction Compensation Based on Recent Knowledge of Dynamic Friction." *Automatica*, Vol. 20, No. 6, 1984.